J. Lindberg, K. Lindfors, T. Setälä, M. Kaivola, and A. T. Friberg. 2004. Spectral analysis of resonant transmission of light through a single sub-wavelength slit. Optics Express, volume 12, number 4, pages 623-632.

Spectral analysis of resonant transmission of light through a single sub-wavelength slit

J. Lindberg[1], K. Lindfors[1], T. Setälä[1], M. Kaivola[1], and A. T. Friberg[2]

[1] *Department of Engineering Physics and Mathematics, Helsinki University of Technology, P.O. Box 2200, FIN-02015 HUT, Finland*

[2] *Department of Microelectronics and Information Technology, Royal Institute of Technology, SE-164 40 Kista, Sweden*

jlindber@cc.hut.fi

Abstract: We analyze the spectral properties of resonant transmission of light through a sub-wavelength slit in a metal film. We show that the enhanced transmission can be understood in terms of interfering surface-wave-like modes propagating in the slit. We characterize the effect of geometrical and material properties of the slit on the transmission spectrum. Furthermore, we show that the wavelength of the transmission resonance strongly depends on the surrounding medium. This effect may be utilized in sensors, imaging, and the detection of, e.g. biomolecules.

OCIS codes: (050.1960) Diffraction theory, (240.6690) Surface waves, (110.1220) Apertures, (230.7390) Waveguides, planar.

References and links

1. T. W. Ebbesen, H. J. Lezec, H. F. Ghaemi, T. Thio, and P. A. Wolff, "Extraordinary optical transmission through sub-wavelength hole arrays," Nature **391,** 667–669 (1998).
2. T. Thio, K. M. Pellerin, R. A. Linke, H. J. Lezec, and T. W. Ebbesen, "Enhanced light transmission through a single subwavelength aperture," Opt. Lett. **26,** 1972–1974 (2001).
3. F. Yang and J. R. Sambles, "Resonant Transmission of Microwaves through a Narrow Metallic Slit," Phys. Rev. Lett. **89,** 063901 (2002).
4. P.-K. Wei, H.-L. Chou, and W.-S. Fann, "Optical near field in nanometallic slits," Opt. Express **10,** 1418–1424 (2002), http://www.opticsexpress.org/abstract.cfm?URI=OPEX-10-24-1418.
5. B. Dragnea, J. M. Szarko, S. Kowarik, T. Weimann, J. Feldmann, and S. R. Leone, "Near-Field Surface Plasmon Excitation on Structured Gold Films," Nano Lett. **3,** 3–7 (2003).
6. U. Schröter and D. Heitmann, "Surface-plasmon-enhanced transmission through metallic gratings," Phys. Rev. B **58,** 15419–15421 (1998).
7. J. A. Porto, F. J. García-Vidal, and J. B. Pendry, "Transmission Resonances on Metallic Gratings with Very Narrow Slits," Phys. Rev. Lett. **83,** 2845–2848 (1999).
8. E. Popov, M. Nevière, S. Enoch, and R. Reinisch, "Theory of light transmission through subwavelength periodic hole arrays," Phys. Rev. B **62,** 16100–16108 (2000).
9. L. Salomon, F. Grillot, A. Zayats, and F. de Fornel, "Near-Field Distribution of Optical Transmission of Periodic Subwavelength Holes in a Metal Film," Phys. Rev. Lett. **86,** 1110–1113 (2001).
10. L. Martín-Moreno, F . J. García-Vidal, H. J. Lezec, K. M. Pellerin, T. Thio, J. B. Pendry, and T. W. Ebbesen, "Theory of Extraordinary Optical Transmission through Subwavelength Hole Arrays," Phys. Rev. Lett. **86,** 1114–1117 (2001).
11. Ph. Lalanne, J. P. Hugonin, S. Astilean, M. Palamaru, and K. D. Möller, "One-mode model and Airy-like formulae for one-dimensional metallic gratings," J. Opt. A: Pure Appl. Opt. **2,** 48–51 (2000).
12. S. Astilean, Ph. Lalanne, and M. Palamaru, "Light transmission through metallic channels much smaller than the wavelength," Opt. Commun. **175,** 265–273 (2000).

#3586 - $15.00 US Received 23 December 2003; revised 10 February 2004; accepted 11 February 2004

13. Q. Cao and Ph. Lalanne, "Negative Role of Surface Plasmons in the Transmission of Metallic Gratings with Very Narrow Slits," Phys. Rev. Lett. **88,** 057403 (2002).
14. S. Collin, F. Pardo, R. Teissier, and J.-L. Pelouard, "Strong discontinuities in the complex photonic band structure of transmission metallic gratings," Phys. Rev. B **63,** 033107 (2001).
15. M. M. Treacy, "Dynamical diffraction in metallic optical gratings," Appl. Phys. Lett. **75,** 606–608 (1999).
16. M. M. Treacy, "Dynamical diffraction explanation of the anomalous transmission of light through metallic gratings," Phys. Rev. B **66,** 195105 (2002).
17. Y. Takakura, "Optical Resonance in a Narrow Slit in a Thick Metallic Screen," Phys. Rev. Lett. **86,** 5601–5603 (2001).
18. A. P. Hibbins, J. R. Sambles, and C. R. Lawrence, "Gratingless enhanced microwave transmission through a subwavelength aperture in a thick metal plate," Appl. Phys. Lett. **81,** 4661–4663 (2002).
19. F. J. García-Vidal, H. J. Lezec, T. W. Ebbesen and L. Martín-Moreno, "Multiple Paths to Enhance Optical Transmission through a Single Subwavelength Slit," Phys. Rev. Lett. **90,** 213901 (2003).
20. F. I. Baida, D. Van Labeke, and B. Guizal, "Enhanced Confined Light Transmission by Single Subwavelength Apertures in Metallic Films," Appl. Opt. **42,** 6811–6815 (2003).
21. H. F. Schouten, T. D. Visser, D. Lenstra, and H. Blok, "Light transmission through a subwavelength slit: Waveguiding and optical vortices," Phys. Rev. E **67,** 036608 (2003).
22. H. F. Schouten, T. D. Visser, G. Gbur, D. Lenstra, and H. Blok, "Creation and annihilation of phase singularities near a sub-wavelength slit," Opt. Express **11,** 371–380 (2003), http://www.opticsexpress.org/abstract.cfm?URI=OPEX-11-4-371.
23. W. L. Barnes, A. Dereux, and T. W. Ebbesen, "Surface plasmon subwavelength optics," Nature **424,** 824–830 (2003).
24. A. V. Zayats and I. I. Smolyaninov, "Near-field photonics: surface plasmon polaritons and localized surface plasmons," J. Opt. A: Pure Appl. Opt. **5,** S16–S50 (2003).
25. J. Homola, S. S. Yee, and G. Gauglitz, "Surface plasmon resonance sensors: review," Sensors and Actuators B **54,** 3–15 (1999).
26. J. J. Mock, D. R. Smith, and S. Schultz, "Local Refractive Index Dependence of Plasmon Resonance Spectra from Individual Nanoparticles," Nano Lett. **3,** 485–491 (2003).
27. A. D. McFarland and R. P. Van Duyne, "Single Silver Nanoparticles as Real-Time Optical Sensors with Zeptomole Sensitivity," Nano Lett. **3,** 1057–1062 (2003).
28. T. Kalkbrenner, M. Ramstein, J. Mlynek, and V. Sandoghdar, "A single gold particle as a probe for apertureless scanning near-field optical microscopy," J. Microsc. **202,** 72–76 (2001).
29. M. Moskovits, "Surface-enhanced spectroscopy," Rev. Mod. Phys. **57,** 783–826 (1985).
30. D. Maystre, "Integral Methods," in *Electromagnetic Theory of Gratings*, R. Petit, ed. (Springer-Verlag, Berlin, 1980), pp. 63–100.
31. M. Nieto-Vesperinas, *Scattering and Diffraction in Physical Optics* (Wiley, New York, 1991).
32. C. M. Kelso, P. D. Flammer, J. A. DeSanto, and R. T. Collins, "Integral equations applied to wave propagation in two dimensions: modeling the tip of a near-field scanning optical microscope," J. Opt. Soc. Am. A **18,** 1993–2001 (2001).
33. J. Wiersig, "Boundary element method for resonances in dielectric microcavities," J. Opt. A: Pure Appl. Opt. **5,** 53–60 (2003).
34. P. A. Knipp and T. L. Reinecke, "Boundary-element method for the calculation of electronic states in semiconductor nanostructures," Phys. Rev. B **54,** 1880–1891 (1996).
35. L. Ram-Mohan and L. Ramdas *Finite Element and Boundary Element Applications in Quantum Mechanics* (Oxford University Press, Oxford, UK, 2002).
36. P. B. Johnson and R. W. Christy, "Optical Constants of the Noble Metals," Phys. Rev. B **6,** 4370–4379 (1972).
37. I. P. Kaminow, W. L. Mammel, and H. P. Weber, "Metal-Clad Optical Waveguides: Analytical and Experimental Study," Appl. Opt. **13,** 396–405 (1974).
38. E. W. Palik, *Handbook of Optical Constants of Solids* (Academic Press, San Diego, 1985).

1. Introduction

The optical properties of nano-structured metallic thin films have been studied extensively since the discovery of enhanced optical transmission through such a structure by Ebbesen *et al.* [1]. Later, it was observed that the enhanced transmission can occur for a wide variety of hole and slit structures [2–5]. The enhanced transmission in arrays of slits or holes is explained to be due to the surface plasmon polaritons propagating on the film [6–10], or the coupling of incident light into slit waveguide modes [7, 11–14], or it can be understood within the framework of dynamical diffraction theory [15, 16]. The difference between the transmission properties of holes and slits is discussed in Ref. [8]. When dealing with a single slit the resonant transmis-

#3586 - $15.00 US Received 23 December 2003; revised 10 February 2004; accepted 11 February 2004

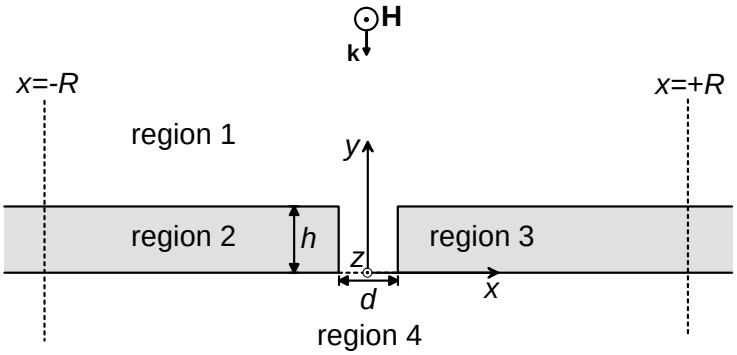

Fig. 1. Model geometry of a nanoslit of width d in a metal film of thickness h. A p-polarized (transverse magnetic) plane wave is normally incident on the structure.

sion of light has been connected to Fabry-Pérot-like resonances [3, 17, 18] and a surface wave propagating within the slit [4]. The possibility to control the directionality of the transmitted light by corrugating the metal film has also been explored [18–20] as well as the influence of optical vortices on the enhancement of transmission [21, 22].

Nanostructured metallic films and their transmission properties are important for both fundamental studies of light-matter interaction and for developing photonic devices based on surface waves, particularly, on surface plasmons. Surface plasmons have shown great potential for applications in sub-wavelength optics with components such as reflectors and switches having already been demonstrated [23, 24]. In addition, the sensitivity of plasmon resonances on the surrounding environment has been exploited in various sensor [25–27] and imaging [28] applications. The resonances have also been made use of in surface-enhanced spectroscopy [29].

In this paper, we calculate and analyze the transmission spectrum of p-polarized (transverse magnetic) light through a single sub-wavelength slit in a metal film. We employ a rigorous boundary-integral method [30–35], in which the optical response of the metal is modelled using a realistic wavelength-dependent refractive index. We show that the enhanced transmission can be understood in terms of interfering waveguide modes that propagate in the slit. Furthermore, we propose to use the transmission resonance of a single sub-wavelength slit as a sensor for detecting small changes in the refractive index of the surrounding medium. The sensor could be used, for instance, to detect biological molecules. By employing modern methods of microfabrication such a sensor could be integrated in different lab-on-chip applications.

The paper is organized as follows: in Section 2 the boundary-integral method is briefly outlined. The results of our calculations of the transmittance properties of the nanostructure are presented and discussed in Section 3, where the suitability of metallic sub-wavelength slits for sensor applications is also examined. The main conclusions are summarized in Section 4.

2. Boundary-integral method

The model geometry representing a metallic nanoslit is depicted in Fig. 1. The structure, which consists of four distinct regions, is uniform in the z-direction and the medium in each region is assumed to be linear, homogeneous, and isotropic. A p-polarized monochromatic plane wave with wavevector $\mathbf{k}$ is normally incident on the structure from above ($y > 0$).

The electromagnetic field in a 2D geometry can be represented as a superposition of an s-polarized (transverse electric, TE) and a p-polarized (transverse magnetic, TM) component. For the s-polarized wave, the single electric field component points in the z-direction whereas

#3586 - $15.00 US Received 23 December 2003; revised 10 February 2004; accepted 11 February 2004

for the *p*-polarized wave a *z*-oriented magnetic field component is used. For both polarizations the electromagnetic field is governed by the 2D scalar Helmholtz equation

$$(\nabla^2 + k_0^2 n^2)\psi(\mathbf{r}) = 0, \tag{1}$$

where $\psi(\mathbf{r})$ denotes the (complex) amplitude of the electric (*s* polarization) or the magnetic field (*p* polarization). Further, $k_0 = 2\pi/\lambda_0$ is the wave number of the field of vacuum wavelength λ_0, n is the refractive index of the medium, and $\mathbf{r} = (x,y)$. In this work we make use of a numerical procedure known as the boundary-integral method, to solve Eq. (1) in the arrangement of Fig. 1. Below we briefly outline the method; for a more comprehensive presentation see, e.g., Refs. [30–35].

The solution of the Helmholtz equation in each homogeneous region of the model geometry can be expressed as a boundary integral

$$\psi_l(\mathbf{r}) = \oint_{s_l} \left\{ G_l(\mathbf{r},\mathbf{r}') \left[\hat{n}\cdot\nabla'\psi_l(\mathbf{r}')\right] - \psi_l(\mathbf{r}') \left[\hat{n}\cdot\nabla' G_l(\mathbf{r},\mathbf{r}')\right] \right\} \mathrm{d}s', \tag{2}$$

where the region is labelled by l (l=1,2,3,4), and $\hat{n}$ denotes the outward unit vector normal to the curve s_l, which encloses the region. The Green function $G_l(\mathbf{r},\mathbf{r}')$, which satisfies the inhomogeneous 2D Helmholtz equation with a delta-function source term, is explicitly given by

$$G_l(\mathbf{r},\mathbf{r}') = \frac{i}{4} H_0^{(1)}(k_0 n_l |\mathbf{r}-\mathbf{r}'|), \tag{3}$$

where n_l is the refractive index of region l and $H_0^{(1)}$ is the zero-order Hankel function of the first kind, and $\mathbf{r}$ and $\mathbf{r}'$ refer to the field and source points, respectively.

None of the regions in the slit geometry is closed. However, to employ the boundary-integral method, the domains must be closed. We therefore adopt the following procedures (see Ref. [32]): The boundaries separating regions 1 and 2, (1 and 3) and regions 2 and 4 (3 and 4), are extended from $x = -R$ ($x = +R$) to $x = -\infty$ ($x = +\infty$). Domains 2 and 3 are then closed with vertical segments at $x = -\infty$ and $x = +\infty$, respectively, and infinite semicircles are used to close domains 1 and 4. For points in region 1, the integral over the semicircle gives the incident field [32], whereas the integral over the semicircle in region 4 vanishes due to the fact that the field is required to satisfy the Sommerfeld radiation condition.

Calculation of the field inside a closed region using the boundary-integral method requires the knowledge of the field and its normal derivative on the boundary. The boundary values are obtained by taking the limit of Eq. (2) as the field point $\mathbf{r}$ approaches the boundary. The Green function and its normal derivative are singular when the field and source point coincide. The singularity of the Green function is integrable, whereas its normal derivative is treated by deforming the contour with an arc of radius ε around the singular point and taking the limiting value as ε goes to zero (see e.g. Ref. [35]). The boundaries in the interval $-R \le x \le +R$ are then discretized and the boundary conditions for the electric and magnetic fields are employed to relate the field and its normal derivative for adjacent regions. Contributions from the upper boundaries for $|x| > R$ are calculated numerically assuming that the field far away from the slit is the sum of normally incident and reflected plane waves. On the lower boundaries the field is assumed to be zero for $|x| > R$, which means that no power flows directly through the film. After the contributions from the extended upper boundaries are taken into account, the field and its normal derivative on the boundary are obtained by solving the ensuing matrix equation [32]. The field inside the closed region can then be calculated from Eq. (2). We note that in the case of *p*-polarized incident light, where the magnetic field is solved using the boundary-integral method, the electric field is obtained from the Maxwell equations.

#3586 - $15.00 US Received 23 December 2003; revised 10 February 2004; accepted 11 February 2004

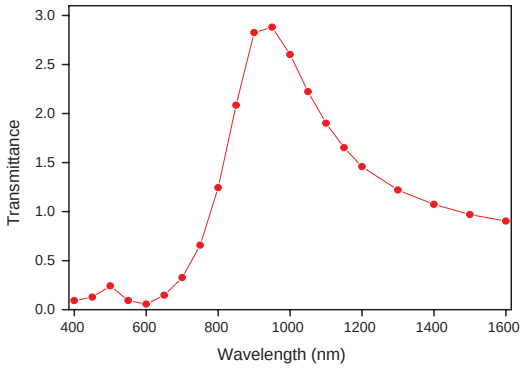

Fig. 2. Transmittance spectrum of a 40 nm wide slit in a gold film with a thickness of 200 nm.

In the following section, we analyze the transmittance properties of *p*-polarized light through the slit. For this purpose, we use the following definition for the transmittance T [21]:

$$T \equiv \frac{\int_{\text{slit}} S_n \mathrm{d}A + \int_{\text{film}} (S_n - S_n^{(\text{trans})}) \mathrm{d}A}{\int_{\text{slit}} S_n^{(\text{inc})} \mathrm{d}A}, \tag{4}$$

where S_n, $S_n^{(\text{inc})}$, and $S_n^{(\text{trans})}$ are the normal components of the time-averaged Poynting vector of the total field, the Poynting vector of the incident field and the Poynting vector of the transmitted field in the absence of the slit, respectively. The differential surface element is denoted by dA and the surface normal is in the direction of negative y-axis. The two integrals in the numerator of Eq. (4) are evaluated over the lower surface (i.e. the plane $y = 0$) of the metal film. Since we have assumed above that no power flows through the film, $S_n^{(\text{trans})}$ is zero. The integral in the nominator of Eq. (4) is used to normalize the transmitted power to the power incident on the slit.

3. Results

Figure 2 shows the calculated transmittance spectrum of a 40 nm wide slit in a gold film with a thickness of 200 nm. The material in region 1 is air ($n = 1.0$) and in region 4 glass with refractive index $n = 1.52$, which is assumed to be constant for all wavelengths. For the refractive index of gold we use the values of Ref. [36]. Two resonance peaks are observed in the transmittance spectrum. In this work, we focus on characterizing the dependence of the main resonance at a wavelength of approximately 950 nm on various geometrical and material parameters. Our results will illustrate that the observed peak in the transmittance spectrum is a morphological resonance due to the excitation of a propagating TM mode in the metal slit. For *s*-polarized light, no resonances in the transmittance spectrum are observed in this case. This is in accordance with the fact that in two dimensional planar waveguide all TE modes have a finite cutoff unlike the lowest TM mode [37].

As a first step, in order to obtain insight into the nature of the transmittance resonances of sub-wavelength slits, we calculate the transmittance spectrum for three different film metals; Al, Au, and Ag. Figure 3 displays the calculated transmission spectra for a 40 nm wide slit in

#3586 - $15.00 US Received 23 December 2003; revised 10 February 2004; accepted 11 February 2004

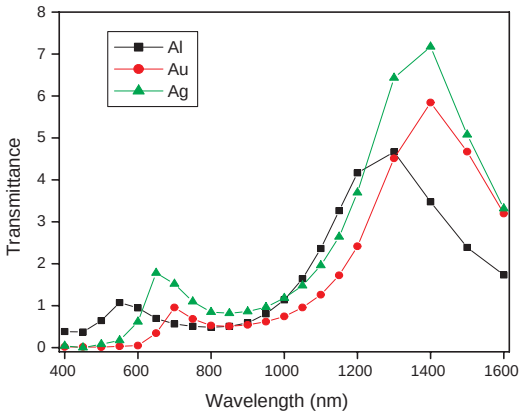

Fig. 3. Transmittance spectra for a 40 nm wide slit in aluminum, gold and silver films with a thickness of 350 nm.

a metal film of 350 nm thickness on glass. The wavelength dependent values of the refractive index of aluminum are taken from Ref. [38] and those of silver and gold from Ref. [36]. In all three spectra of Fig. 3 one can clearly observe two distinct peaks, a smaller one at the visible wavelengths and a larger one in the infrared spectral region. At the stronger resonance the transmitted power through the slit is several times higher than the power that is incident on the slit. Moreover, the three transmittance spectra are all similar in shape indicating that the phenomenon leading to resonant transmission does not strongly depend on the properties of the metal, but is rather a geometrical effect. Our results show that as the skin depth of the metal increases (smallest for aluminum and largest for gold) the resonance peak is shifted to the red. The process leading to the resonance can be qualitatively understood by considering the slit as a planar waveguide. The lowest order transverse magnetic mode in the planar metallic waveguide has no cut off and is known to exhibit surface-wave-like behavior [37]. This waveguide mode is reflected at both ends of the slit and thus the slit acts like a resonator, for which the condition of the resonance is determined by the propagation constant of the mode. We have calculated the propagation constants of the waveguide mode as a function of the waveguide width and cladding material [37]. From this analysis, we observe that the losses for the waveguide mode are higher at visible frequencies than in the near-infrared spectral region, which accounts for the difference in the transmittance at the two resonances of Fig. 3. Moreover, in a planar metallic waveguide the effective refractive index increases with increasing skin depth of the material. This is consistent with the observed red shift of the resonance wavelength λ_0 of the incident field, since the surface wave wavelength scales as $\lambda = \lambda_0/n_{\text{eff}}$, where n_{eff} is the effective index of refraction.

To further study the origin of the resonances, we examine the intensity distribution ($|E|^2$) of the field on resonance and off resonance. The field distributions were calculated for a slit width of 40 nm in a gold film with a thickness of 200 nm, and are shown in Figs. 4(a) and 4(b), for the off-resonance ($\lambda = 600$ nm) and on-resonance ($\lambda = 950$ nm) case, respectively. The time-averaged Poynting vectors are shown as arrows. One observes that in the off-resonance case the direction of the power flow on the edges above the metal film is away from the slit, whereas on the resonance the slit is a power sink. Furthermore, at resonance, the field is localized to the

#3586 - $15.00 US Received 23 December 2003; revised 10 February 2004; accepted 11 February 2004

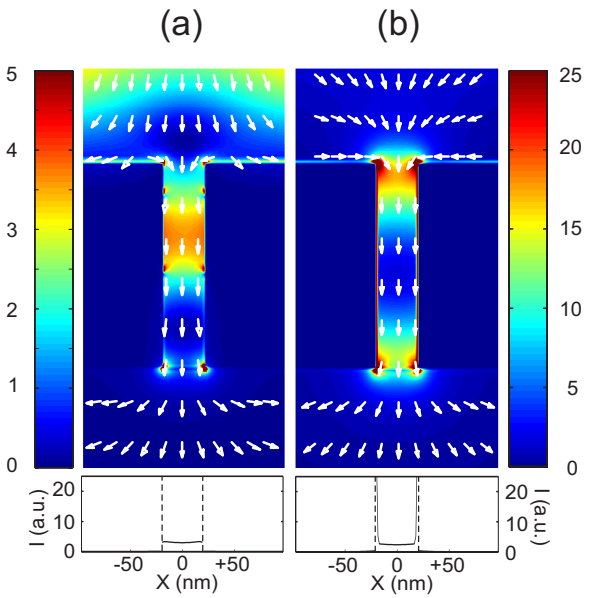

Fig. 4. Intensity distribution ($|E|^2$) around a 40 nm wide slit in a gold film with thickness of 200 nm: (a) off resonance ($\lambda = 600$ nm), and (b) at resonance ($\lambda = 950$ nm). The intensity is normalized to the incident field intensity. The scale in (b) is different from that in (a) so that the details of the intensity distribution can be more clearly seen. The time-averaged Poynting vectors are shown as arrows. The insets in (a) and (b) show the intensity distribution near the center of the slit ($y \approx 100$ nm). The material interface is shown as dashed line.

metal surface inside the slit which is not observed in the off-resonance case. This is particularly clearly seen in the insets of Fig. 4, which show the cross-sections of the intensity distributions near the center ($y \approx 100$ nm) of the slit. In the middle of the slit the intensity is fairly similar in the resonance and off-resonance cases. The differences in the intensity are localized within a distance of only 4 nm from the slit walls. These results further strengthen the hypothesis that the resonant transmission of a metal slit is due to the excitation of a waveguide mode with surface-wave characteristics.

By changing the thickness of the metal film, we change the length of the resonant cavity and thus expect a corresponding shift in the spectral position of the resonance peaks. The transmittance spectra for a 40 nm wide slit in gold films of thicknesses 200 nm, 275 nm and 350 nm are presented in Fig. 5. We observe the expected shift of the resonance peak towards longer wavelengths as the thickness of the film increases. In addition, the resonance peak becomes more pronounced as the losses of the waveguide mode decrease, as discussed earlier.

Next, we consider the effect of the slit width on the transmittance spectrum. In Fig. 6 are presented the transmittance spectra for slit widths of 100 nm, 50 nm, 25 nm, and 15 nm in a gold film of thickness 200 nm. It is seen that as the slit width is reduced, the resonance peak becomes significantly narrower. Furthermore, one notices that the transmittance increases and that the resonance peak shifts to the red with decreasing slit width. As the waveguide becomes narrower the real part of the propagation constant of the waveguide mode increases. This corresponds to a higher real part of the effective index of refraction, and thus to a longer optical length of the cavity, which explains the red shift of the resonance peak. Furthermore, as

#3586 - $15.00 US Received 23 December 2003; revised 10 February 2004; accepted 11 February 2004

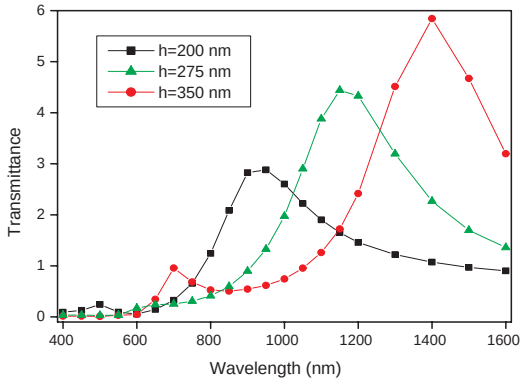

Fig. 5. Transmittance spectra for a 40 nm wide slit in gold films of various thicknesses.

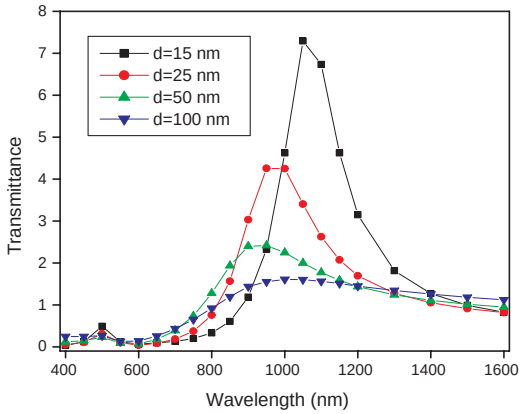

Fig. 6. Transmittance spectra for various slit widths in a gold film with a thickness of 200 nm.

the real part of the effective index of refraction increases the reflectivity of the waveguide ends also increases. For decreasing slit widths, the finesse of the resonator therefore increases and the transmission resonances become markedly narrower.

So far, we have analyzed the changes in the transmittance spectrum as a function of the film material and slit geometry. In order to find out the dependence of the transmittance resonance on the material in and above the slit (region 1 in Fig. 1) we fix the material and the geometry of the structure to a gold film with a thickness of 200 nm and a slit width of 15 nm. We have calculated the transmittance spectra for air ($n = 1.0$), water ($n = 1.33$), glass ($n = 1.52$), and oil ($n = 1.56$). The results are shown in Fig. 7. As the refractive index of the slit medium increases, the resonance undergoes a significant red shift. As already pointed out, the losses of the waveguide mode in the visible spectral region are higher than in the near-infrared leading to

#3586 - $15.00 US Received 23 December 2003; revised 10 February 2004; accepted 11 February 2004

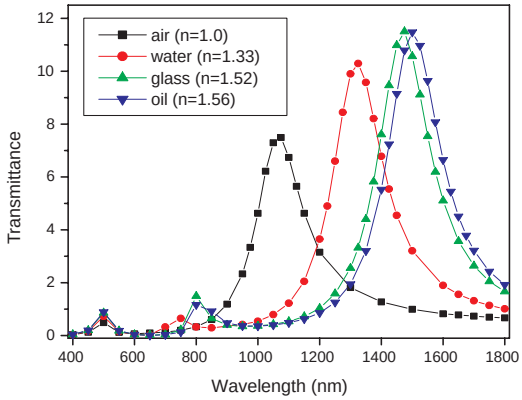

Fig. 7. Transmittance spectra for a 15 nm wide slit in a 200 nm thick gold film as the material within the slit is varied.

much reduced resonances around $\lambda = 500$ nm and $\lambda = 800$ nm. In contrast to the dominating resonance, these minor transmission peaks at $\lambda = 500$ nm and $\lambda = 800$ nm shift much less as the index of refraction of the surrounding medium is increased. This observation can be understood based on the analysis of the planar waveguide propagation constant, which shows high dispersion at around $\lambda = 500$ nm, i.e., a small change in the wavelength leads to a large change in the propagation constant. Thus only a small shift in the wavelength is enough to satisfy the resonance condition for the different materials of Fig. 7.

The significant shift of the transmission resonance can be used to monitor changes in the surrounding medium. To quantify the sensitivity of the position of the resonance on the index of refraction of the slit material we have extracted the positions of the dominating resonance peaks as a function of the index of refraction. The results are shown in Fig. 8. The positions of the peaks are obtained by fitting a Lorentzian profile to the resonance curves of Fig. 7. As can be seen from Fig. 8, the shift of the resonance peak scales linearly as a function of the refractive index of the material in the slit. This behavior shows the potential of the resonant metallic slit for sensor applications. Our results indicate that for the particular configuration considered here, a change of 0.01 in the index of refraction, would cause a change of 8 nm in the position of the resonance peak. This sensitivity compares favorably with sensors based on plasmon resonant silver nanoparticles [27], for which a similar change results in a spectral shift on the order of 2 nm. Furthermore, the slit system can readily be optimized for a specific detection scheme by adjusting the geometry of the structure.

4. Conclusions

We have characterized the optical properties of a sub-wavelength slit in a metal film using a rigorous method to solve the scattering problem. In this work, we have employed experimentally determined material parameters to analyze the resonant transmission of light through the slit. The analysis shows that there exists a strong resonance in the transmission spectrum of the structure in the near-infrared spectral region. The calculations show that the transmission resonance is a geometric effect resulting from the constructive interference of waveguide modes propagating within the slit. The propagation constant of the mode depends only weakly on the dielectric constant of the metal so that the transmission properties of the structure are similar

#3586 - $15.00 US Received 23 December 2003; revised 10 February 2004; accepted 11 February 2004

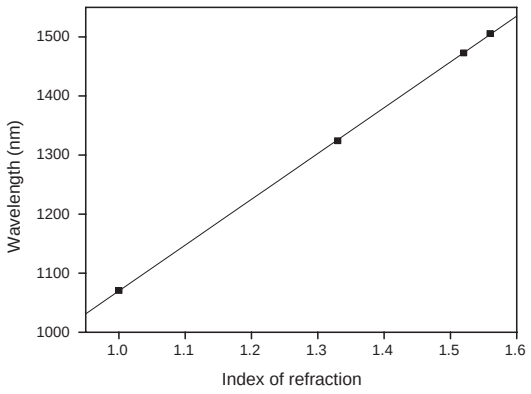

Fig. 8. Resonance peak positions as a function of index of refraction. The squares correspond to calculated data for different materials within the slit and the line is a linear fit to the data.

for Al, Ag, and Au. In contrast, the geometry of the structure considerably affects the transmission spectrum. By decreasing the width of the slit the quality factor of the resonance can be increased, whereas the position of the resonance can be shifted by adjusting the thickness of the metal film. Thus the transmission spectrum can be flexibly tuned for different applications. We have shown that the position of the transmission resonance depends strongly on the refractive index of the material within the slit. This effect may be used in applications including sensors, imaging, and the detection of, e.g. biomolecules. We are currently preparing experiments to realize a sensor based on the effect.

Acknowledgments

The authors acknowledge financial support from the Academy of Finland, and A. T. F. also from the Swedish Research Council. K. L. is grateful for financial support from the Finnish Graduate School of Modern Optics and Photonics, the Vilho, Yrjö and Kalle Väisälä Fund, the Finnish Foundation of Technology, and the Ella and Georg Ehrnrooth Foundation. J. L. acknowledges a grant from the Jenny and Antti Wihuri Fund and T. S. from the Finnish Cultural Foundation.

#3586 - $15.00 US Received 23 December 2003; revised 10 February 2004; accepted 11 February 2004